AGROTHERMIE – DESIGN AND TESTING OF A NOVEL HYDRAULICALLY-ACTUATED, LOCALLY VIBRATING PLOUGH

Jianbin Liu*[1], Benjamin Beck[1], Jakob Münch[2], André Grosa[2], Roman Kahle[2], Prof. Dr.-Ing. Jürgen Weber[1], Prof. Dr.-Ing. habil. Thomas Herlitzius[2]

[1]*Institute of Mechatronic Engineering – Chair of Fluid-Mechatronic Systems, Technical University of Dresden, Helmholtzstrasse 7a, 01069 Dresden*
[2]*Institute of Natural Materials Technology – Agricultural Systems and Technology, Technical University of Dresden, Bergstrasse 120, 01069 Dresden*
* Corresponding author: Tel.: +49 351 46338609; E-mail address: jianbin.liu@tu-dresden.de

ABSTRACT

Economic utilization of geothermal networks under agricultural surfaces needs large agricultural areas. In order to exploit the cultivated land more effectively, this paper proposes a novel locally vibrating plough system that employs a hydraulic actuator direct on the plough blade instead of the state of the art external vibration units. Starting with a description of geothermal networks under agricultural surfaces and the construction technology in details, the contribution shows different concepts, the development and test of the most promising solution for imprinting local vibrations at the cutting edge with the goal of traction force reduction. A virtual demonstrator, the test rig set-up and the control concepts are described. Both of the closed-loop simulation and experimental position control of the entire vibration system demonstrate that the novel design has impressive performance improvement. Finally, the integration of the vibration system into a prototype tool is shown and the reduction of the traction force is proven by experiments carried out with a tractor on a testing field.

Keywords: Agrothermie, high frequency, Co-Simulation, OPC UA, traction force

1. INTRODUCTION

Geothermal energy from depth probes in conjunction with heat pumps has been state of the art for several years as an energy efficient heat supply for building heating and hot water production. As a new way of gaining primary energy for the use in heat pumps, underground collector networks have been established in a depth of only about 2 m under agricultural surfaces - an approach called ‘Agrothermie’. As opposed to the geothermal depth probes, those collectors use ambient energy from sources as seepage water or sun radiation onto the ground. Water temperature in these networks typically lies between T_{min}= 2 °C and T_{max} = 10 °C with a temperature rise between input and output of ΔT = 4 °C. This temperature level allows for heating via heat pumps and for direct cooling use. As the water in the collector has the temperature of the surrounding soil, heat losses through dissipation don’t occur. More publications about project ‘Agrothermie’ can be found in [1], [2] and [3].

In order to keep the agricultural fields in good condition, the soil structure must not be destroyed during the building of the collector. Thus, a system has been developed in order to erect those networks in a minimally invasive way. A specially designed tractor plows three parallel pipes into the ground at a time, which are connected to form a network at the edges of the field later on. The width of the implement is only 0.1 m at the surface in order to achieve the least possible soil damage.

Even for a highly specialized machine on bulldozer tracks, the traction force of the pipe laying implement 2 m deep in the ground can exceed the pulling capacity depending on soil parameters. In order to significantly reduce the needed traction force, vibration of the implement can be helpful. As part of the research project, a novel locally vibrating plough system that employs a hydraulic actuator direct on the plough blade has been developed.

2. CONCEPTS OF GENEREATING LOCAL VIBRATION

Periodic oscillations provide the basis for a wide range of applications in vibration technology. These include sieves, vibrating tables and compressors, vibratory mills, vibratory conveyors, testing machines, vibration pumps, shaking chutes, impact drills and dosing conveyors. Crank drives, unbalance exciters, electromagnetic vibration exciters, hydraulic or pneumatic drives generate the oscillating movements for these. The most commonly used types of drive are also assigned to the application cases [4].

Depending on the process, the vibrations must have different characteristics in order to meet the technological requirements in a process-specific and optimal way. This requires drive systems that can excite and amplify the desired vibrations in the best possible way. Hence, the dynamic behaviour of the excited bodies must be taken into account. At the same time, it is often necessary to decouple the vibrations from the environment or the frame [4].

Due to their high power density, hydraulic drives are always used for vibration excitation when large forces are required. This is the case, for example, in construction machinery, where they are used for demolition hammers and vibratory pile drivers.

Hydraulic vibrators also offer the advantage that the vibration frequency can be continuously varied, allowing the system to be adapted to changing soil conditions. Vibrators with resonance-free starting and stopping can also switch the eccentric weights on and off. If the weight is only switched on when the working frequency is reached, it is easy to pass through the resonance frequency of the soil and resonance peaks are avoided. In addition, the amplitude can be continuously controlled, allowing the frequency and amplitude to be optimally adjusted to the geology.

The requirements for local vibration excitation for the installation tool are shown in extracts in Table 1.

Table 1: Requirements for local vibration unit

Category	Description	Demand d / Wish w
Vibration frequency	Variably adjustable 20 – 50 Hz	d
	Adjustable and operated from the carrier machine	w
Vibration amplitude	Variably adjustable 1 – 10 mm and operated from carrier machine	w
Vibration mass	Max. 50 kg	w
Motion path	Variably adjustable	w
Effective direction	Variably adjustable	w
installation space	Max. width 55 mm, partially extendable to 80 mm	d
Valve technology	Robust and cost-effective	w
components	Available on the market	d
system	Easy to install and maintain	w
Actuator system	Hydraulic	d

The systematic development process according to VDI 2221 was used to find a solution. This procedure was applied on all the identified subsystems (namely: kinematics, valve system and actuators) for the local vibration unit. The combination of subsystem solutions defines the morphological box for new system layouts. Hydraulic motors with eccentrics could be ruled out at an early stage due to the high installation space requirements. The resulting solution space is displayed in **Figure 1**. By means of a weighted point evaluation on the basis of the criteria variability of the vibration parameters, design effort, installation space, complexity of the system, operating modes, process forces that can be applied, number of actuators, requirements on the actuating dynamics and robustness, the grey-shaded preferred variant could be determined. The classical valve-controlled cylinder drive with a 4/3 control valve on a constant pressure system is therefore used in the following for vibration excitation and further investigated.

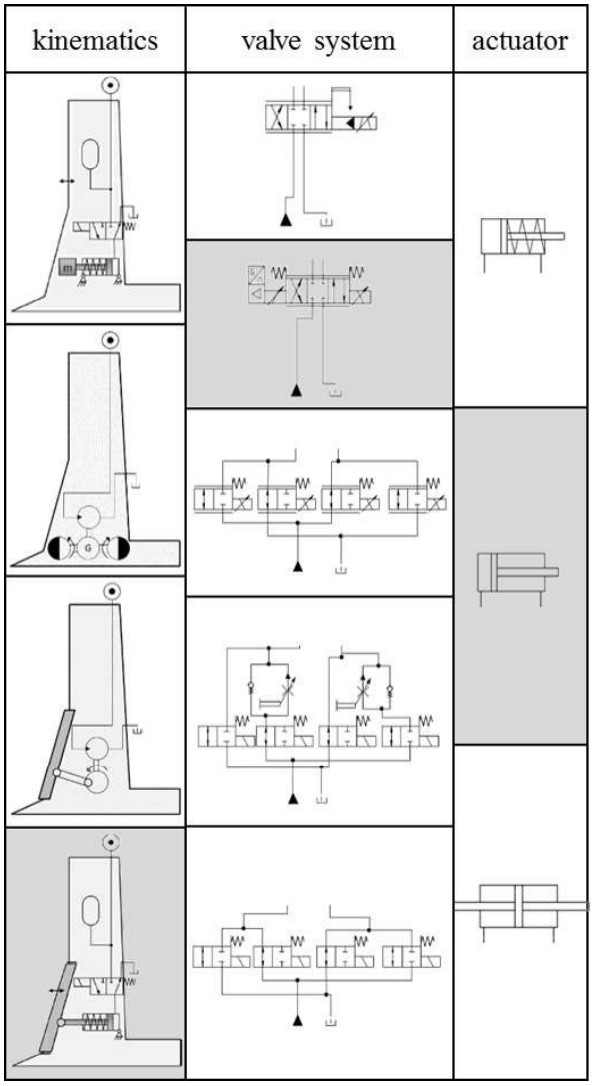

Figure 1: Morphological box and selection of the preliminary concept

3. TEST RIG SETUP AND CONTROL ALGORITHMS

3.1. Mathematical model of hydraulically actuated vibration plough blade

As displayed in **Figure 2**, the hydraulically actuated vibration plough blade system primarily comprises a switching valve, a proportional valve and a hydraulic cylinder with load. The pressure relief valve not only takes charge of system safety, but also holds a constant system pressure of $p_0 = 200$ bar. Because the proportional valve has a small negative overlap in neutral position, it can't hold the position of cylinder without the controller. In order to remedy this defect, a 3/2 switching valve is placed between the proportional valve and pump. For the above reasons, the dynamic property of the system upstream of the proportional valve can be ignored for control development.

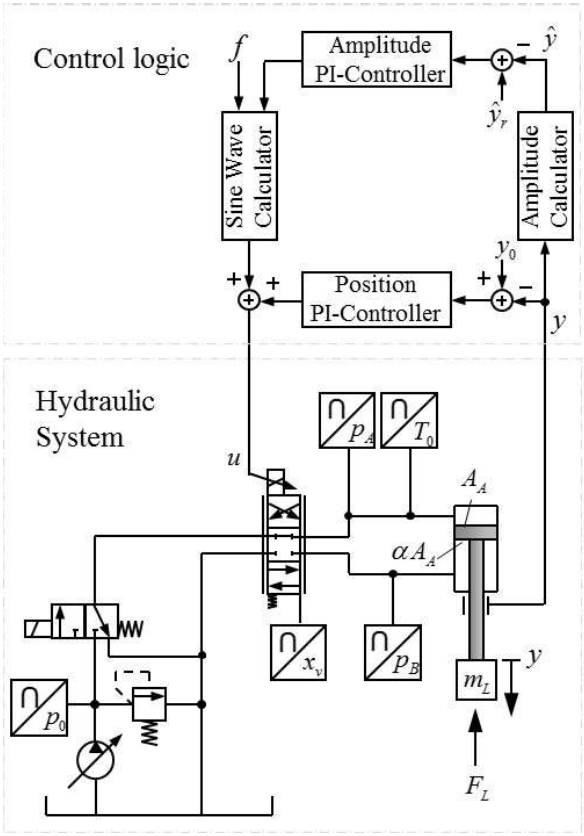

Figure 2: Schematic plan of the hydraulically actuated vibration unit

One of the most important components of the hydraulically actuated vibration unit is the proportional valve, as it must control the volume flow very dynamically and precisely for high frequencies. For the sake of assurance of high dynamics, the characteristic frequency of proportional valve should be at least triple as high as the total system [5]. Therefore, the relationship between input voltage u and displacement for spool valve x_V with electromagnet can be simplified and described as:

$$x_V = K_V \cdot u \tag{1}$$

If the small negative overlap of proportional valve is neglected, according to the operational directions of a hydraulic spool valve and cylinder, the flow rate eq. for valve with zero overlap are obtained as follows:

$$x_V > 0, \quad y > 0:$$
$$\begin{cases} Q_A = A\dot{y} = B \cdot x_V \cdot \sqrt{p_0 - p_A} \\ Q_B = \alpha A\dot{y} = B \cdot x_V \cdot \sqrt{p_B - p_T} \end{cases} \tag{2}$$

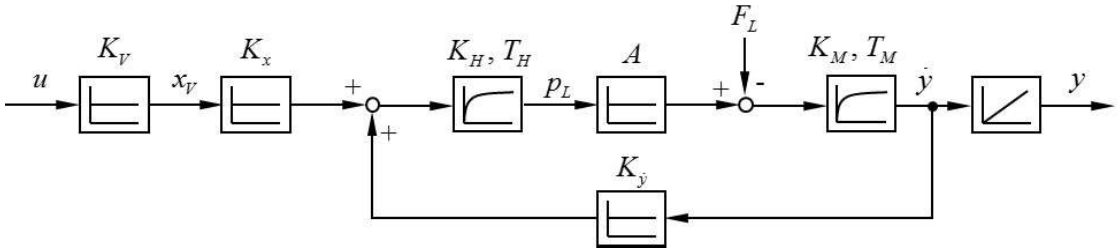

Figure 3: linearized block diagram of the hydraulically actuated vibration plough blade

$$x_V < 0, \qquad y < 0:$$
$$\begin{cases} Q_A = A\dot{y} = B \cdot x_V \cdot \sqrt{p_A - p_T} \\ Q_B = \alpha A\dot{y} = B \cdot x_V \cdot \sqrt{p_0 - p_B} \end{cases} \tag{3}$$

The load pressure p_L for differential cylinder is defined as:

$$p_L = p_A - \alpha p_B \tag{4}$$

According to eq. (2), (3) and (4), mathematical eq. for cylinder chamber pressure p_A and p_B can be obtained on the premise that the system pressure p_0 is constant and tank pressure p_T is zero ($p_0 = const., p_T = 0$):

$$\begin{cases} p_A = \dfrac{p_L + \alpha^3 p_0}{1 + \alpha^3} \\ p_B = \dfrac{(p_0 - p_L)\alpha^2}{1 + \alpha^3} \end{cases} \tag{5}$$

Based on the flow rate characteristics of a hydraulic spool valve, the linearized flow rate eq. for hydraulic zero point ($Q_{A0} = Q_{B0} = 0$, $p_{A0} = p_{B0} = 0$) is given as follows:

$$\begin{cases} Q_A = K_{xA} x_V - K_{pA} p_A \\ Q_B = K_{xB} x_V - K_{pB} p_B \end{cases} \tag{6}$$

If the external leakage is neglected, the leakage can be estimated by:

$$Q_{Le} = K_{Lep}(p_A - p_B) + K_{Le\dot{y}}\dot{y} \tag{7}$$

According to the flow continuity equation, the expression for the pressure change in cylinder chamber can be derived as:

$$\begin{cases} \dot{p}_A = \dfrac{1}{C_A}(Q_A - A\dot{y} - Q_{Le}) \\ \dot{p}_B = \dfrac{1}{C_B}(\alpha A\dot{y} + Q_{Le} - Q_B) \end{cases} \tag{8}$$

The eq. (4) can also be written as:

$$\dot{p}_L = \dot{p}_A - \alpha \dot{p}_B \tag{9}$$

Substituting eq. from (5) to (8) into eq. (9), the first order function for load pressure can be given as:

$$T_H \dot{p}_L + p_L = K_H(K_x x_V + K_{\dot{y}}\dot{y}) \tag{10}$$

with coefficient K_x, coefficient $K_{\dot{y}}$, the hydraulic gain K_H and hydraulic time constant T_H:

$$K_x = \frac{K_{xA}}{C_A} + \frac{\alpha K_{xB}}{C_B}$$

$$K_{\dot{y}} = -\left[\frac{A + K_{Le\dot{y}}}{C_A} + \frac{\alpha(\alpha A + K_{Le\dot{y}})}{C_B}\right]$$

$$K_H = T_H = \frac{1}{\frac{1}{C_A}\left[\frac{K_{pA} + K_{Lep}(1+\alpha^2)}{1+\alpha^3}\right] + \frac{\alpha}{C_B}\left[\frac{K_{Lep}(1+\alpha^2) - K_{pB}\alpha^2}{1+\alpha^3}\right]}$$

According to Newton's second law, the force balance eq. for hydraulic cylinder with load can be described as:

$$m_L\ddot{y} = \Sigma F = Ap_L - d_{\dot{y}}\dot{y} - F_L \tag{11}$$

The second order function for eq. (11) can be expressed as:

$$T_M\ddot{y} + \dot{y} = K_M(Ap_L - F_L) \tag{12}$$

with the mechanical gain K_M and mechanical time constant T_M:

$$K_M = \frac{1}{d_{\dot{y}}}, T_M = \frac{m_L}{d_{\dot{y}}}$$

With the help of eq.(1), (10) and (12), the linearized block diagram of the hydraulically actuated vibration plough blade can be shown in **Figure 3**.

After simplification, the command response from proportional valve input voltage to the actuator-generated displacement can be written as follows:

$$y = \frac{b_{10} \cdot u}{s^2 + a_1 s + a_0} \cdot \frac{1}{s} \tag{13}$$

The corresponding disturbance response can be expressed as follows:

$$y = -\frac{(b_{21}s + b_{20})F_L}{s^2 + a_1 s + a_0} \cdot \frac{1}{s} \quad (14)$$

On the basis of superposition principle, the total system transfer function can be given as follows:

$$y = \frac{b_{10}u - (b_{21}s + b_{20})F_L}{s^2 + a_1 s + a_0} \cdot \frac{1}{s} \quad (15)$$

with the coefficients:

$$a_1 = \frac{T_H + T_M}{T_M T_H}, \quad a_0 = \frac{1 - K_H K_M K_{\dot{y}} A}{T_M T_H}$$

$$b_{10} = K_H K_M K_x K_V A, \quad b_{21} = K_M T_H, \quad b_{20} = K_M$$

It can be seen from command response (13) that in order to acquire a higher amplitude of actuator, it is necessary to input stronger excited signal. According to disturbance response (14), it is concluded that the more load force acts on cylinder, the less amplitude is excited. In summary form (15), the amplitude depends mainly on excited input signal and the acting load force.

4. CONTROL ALGORITHMS

Because the PI or PID controller are unsuitable for the electro-hydraulic system with direct position feedback in high frequency area, a novel control logic has been developed, see **Figure 2**. Firstly, in order to realize the high dynamic requirements, a feed-forward control transmits directly a control signal from a sine wave generator to the proportional valve. Thereby, the valves set voltage for retraction and extension is the same. Because of the different acting areas in each cylinder chamber by using a differential cylinder and the internal leakage, the feed-forward control has difficulties to keep the differential cylinder at the desired position. To compensate this drawback, a closed loop position control with a PI-Controller was introduced. A displacement transducer was mounted inside the cylinder to measure its piston displacement y which can serve as a feedback signal. Compared with the set point y_0, the desired midpoint for the sine wave could be maintained by the controller output. In the meantime, to acquire the actual amplitude of cylinder ŷ, an amplitude calculator was implemented. A PI amplitude controller sets the variable ŷ so that it corresponds to the setpoint input $\hat{y}_r$. The output of the amplitude controller and set frequency f act together as input signals for the sine wave generator. By this way, the amplitude and the frequency of the hydraulically actuated vibrator can be controlled independently. In addition, it is mentioned that the derivative term in the controller was given up for the reason that it amplified process noise from signal which could cause unstable problems in hydraulic system with high frequency.

4.1. Simulation and Test rig results

Simulation Test

With the help of software-in-the-loop testing, the developed algorithms and entire control strategy could be tested within one environment [6, 7], which might reduce risk of integration and improve the reliability of verification in the next phase. Compared with hardware-in-the-loop tests, software-in-the-loop testing is a useful technique at earlier stages of development. It is not necessary to consider the hardware and physical interfaces between controller and plant. Nonetheless, it is inevitable that a coupling layer should be defined. The coupling layer is responsible for exchange of process variables and time synchronisation between controller and simulated model. The coupling layer could be an OPC-UA Server like displayed in **Figure 4**. More specifications about OPC-UA can be found in [8, 9, 10].

The main parameters of simulation model in **Figure 4** are shown in **Table 2**.

Table 2: Main parameters of simulation model

Parameters	Value
Cylinder piston diameter D	40 mm
Cylinder rod diameter d	28 mm
Cylinder max. stroke y_{max}	60 mm
Equivalent load mass m_L	10 kg
Damping coefficient of cylinder $d_{\dot{y}}$	5 Ns/mm
Natural frequency of proportional valve f_V	90 Hz
Damping coefficient of proportional valve d_V	0.75
Hydraulic oil	HLP 46
Cycle time	2 ms

Figure 4 depicts the LabVIEW-SimulationX Co-Simulation with an OPC UA coupling layer. A virtual image of the controller in LabVIEW took

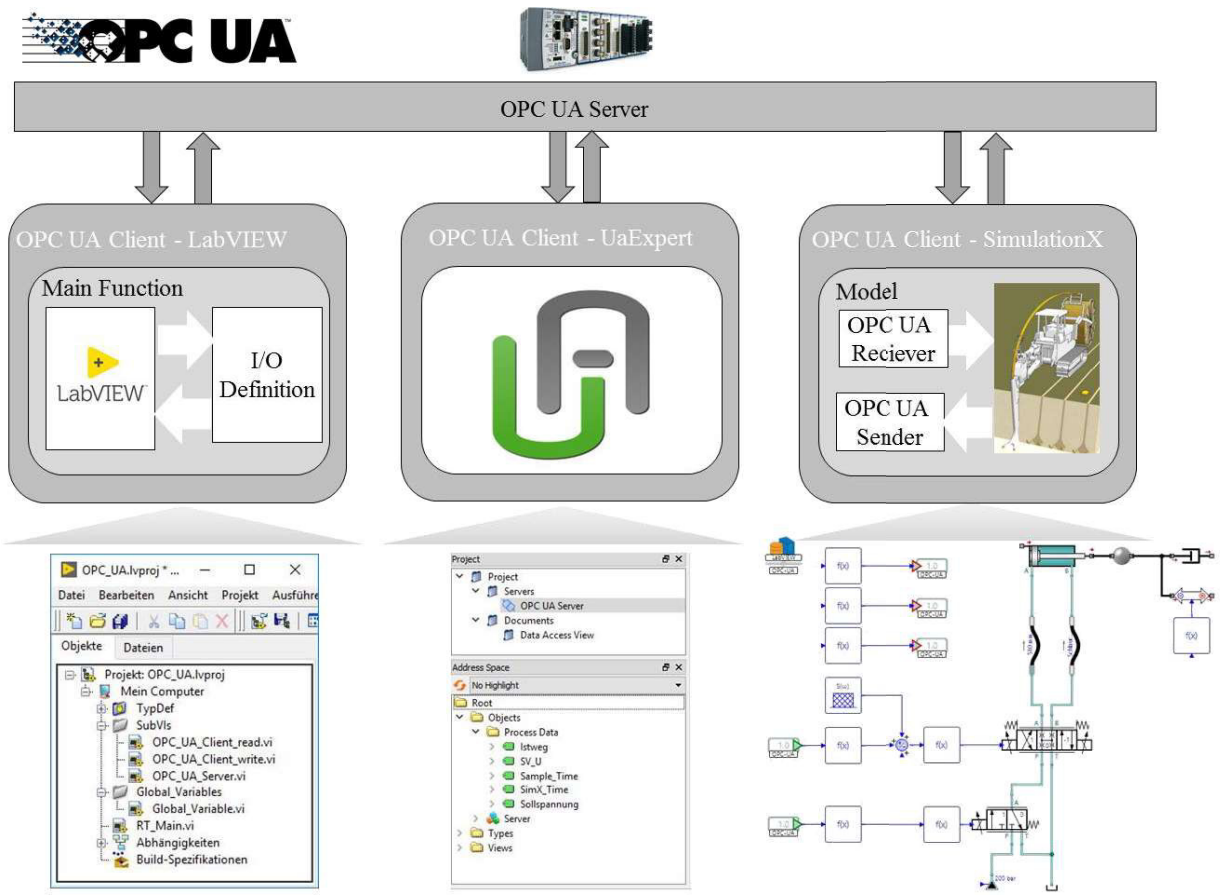

Figure 4: LabVIEW-SimulationX Co-Simulation with OPC UA

over the controlling mission for simulation model in SimulationX. After the definition of the interface, all the relevant input/output signals between virtual controller and simulation model via OPC UA Server were exchanged. The UaExpert was designed as an OPC UA viewer, which supported OPC UA features like browsing OPC UA address space, reading and writing of variable values and UA attributes, monitoring of data changes and events.

Test Rig

To evaluate the theoretical analysis and to validate simulation model, a test rig used to test the hydraulically actuated vibration unit has been set up. According to the schematic plan in **Figure 2**, the experimental set up including pressure relief valve, proportional valve, sensors and load is shown in **Figure 5**. For simplicity, the reactive force from soil was produced by the rubber plates which acted as a load unit. In order to meet the high requirements from control quality, the CompactRIO system with real-time embedded industrial controller was introduced. The developed LabVIEW code from the software-in-the-loop project was adapted and implemented in the CompactRIO system without much effort. All signals were acquired, delivered, demonstrated and stored with the help of this system. Furthermore, in order to realize the high frequency control and reduce the influence from signal noise at the same time, a compromise for sampling time was made, which was set to 2 ms.

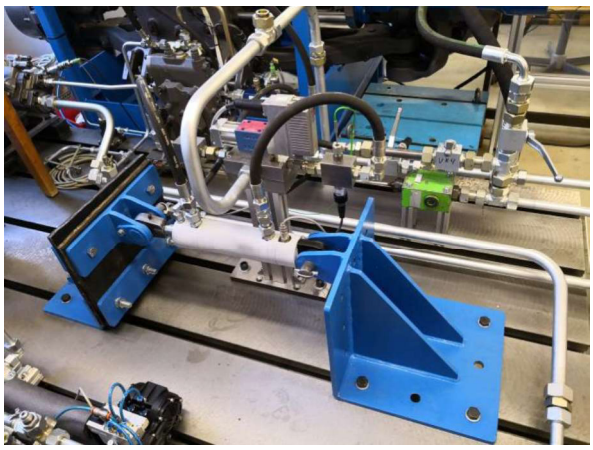

Figure 5: Test rig of hydraulically actuated vibration unit

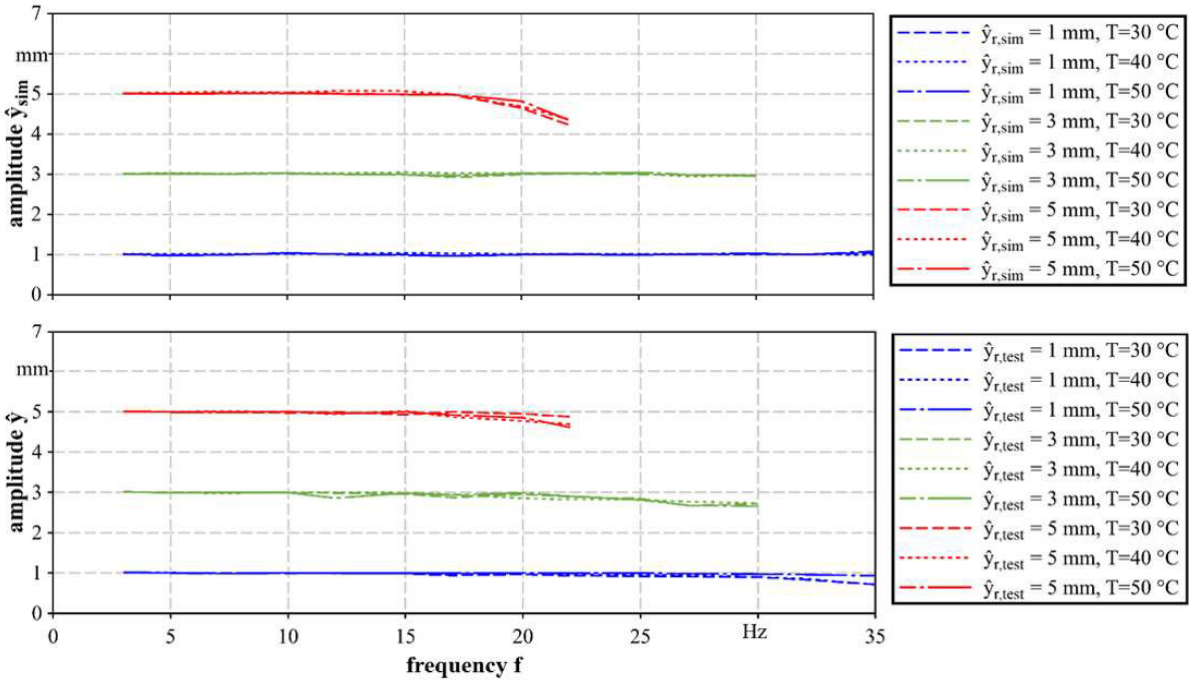

Figure 6: frequency responses between test and simulation at different temperatures

Results and discussion

To test the validity and robustness of the control strategy, a series of tests with the help of the above mentioned Co-Simulation and test rig have been carried out. **Figure 6** presents the experimental results of frequency responses between test and simulation at different temperatures. As a whole, the simulation results are in good agreement with the test results at different temperatures. At the same reference amplitude $\hat{y}_r$, the control strategy brings about a wide frequency bandwidth. The cylinder amplitude $\hat{y}$ will only attenuate at the high frequency until the input voltage for proportional valve reaches limited value. It can also be seen that the higher reference amplitude $\hat{y}_r$ inputs, the less frequency bandwidth is available. The difference between test results and simulation results at high frequency area could attribute to the uncertainties of various parameters in simulation model, especially the frequency characteristic of the proportional valve from data sheet and other non-linearities in the system like friction. For these reasons, the proportional valve in simulation model reaches the minimal input voltage ($u_{min} = -10\,V$) a little earlier. It can also be seen from **Figure 6** how temperatures affect frequency responses under control. As a result, the influence from temperature on frequency response can be almost neglected. In other words, the control system is robust enough to compensate the effect from temperature. It is easy to draw this consistent conclusion not only from simulation but also from test results.

A deficiency of this control strategy is located at the area of low frequency (0 - 3 Hz). There are two main reasons for that: On the one hand, higher noise compared with the input voltage occurs in this area. On the other hand, the cylinder speed at low set frequencies is also low and the drive tends to stick-slip. In order to solve this problem, it is suggested that direct position control with another PI-Controller for the low frequency area could be implemented in the control strategy. Because the machine in reality would never work in this low frequency area, the control strategy in **Figure 2** could be treated as suitable for the real application.

In the process of high frequencies, it is possible that the hydraulic oil can't exchange with tank, which could give rise to heat accumulation and seal failure in cylinder. In order to observe the heat accumulation in cylinder chamber in the meanwhile, a durability test has been carried out. For this purpose, a classic two point control for tank temperature was adopted and its desired value was set to 40 °C ± 2 °C at the central cooling unit of the test rig. If the temperature equaled or exceeded the threshold 42 °C, the cooling system turned on until

temperature dropped below the threshold 38 °C and at that point the system turned back off. It is clear from **Figure 7** that the temperature in cylinder chamber remained relative constant and the tank temperature could still exert influence on it. It's no doubt that the heat accumulation could be prevented by the control of tank temperature.

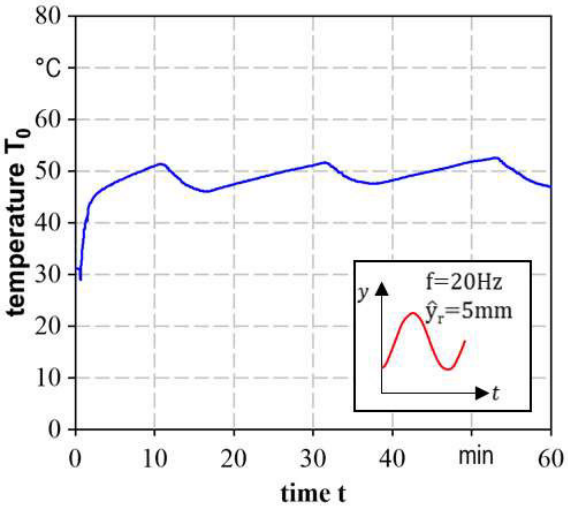

Figure 7: Durability test for temperature in cylinder chamber

5. PLOUGH INTEGRATION AND TRACTOR TEST

In order to analyse influence of the amplitude $\hat{y}$, frequency f and midpoint y_0 on the traction force, the hydraulically actuated vibration plough blade has been constructed and integrated on a tractor. Because of the ongoing patent application, the corresponding results will be published later.

In order to identify the reduction of traction force, two kind of field tests have been completed. At first, a field test began with constant frequency $f = 15\,Hz$ and an amplitude of $\hat{y}_r = 5\,mm$. During the field test, the excitation would be given up at a certain time ($t = 760\,s$). The corresponding measurement results are shown in **Figure 8**. Compared to the mean traction force of $F_{T,mean,1} = 28.3\,kN$ with excitation in range of $\Delta t(f = 15\,Hz)$, the mean traction force without excitation ($\Delta t(f = 0\,Hz)$) has increased to $F_{T,mean,2} = 31.6\,kN$. The traction force has been reduced by 11.8 % with the help of the hydraulically actuated vibration plough blade.

The other field test was carried out with variable frequencies up to $20\,Hz$ and a constant amplitude of $\hat{y}_r = 5\,mm$. In **Figure 9**, the relationship between the traction force and frequency is shown. Nevertheless, it is not one

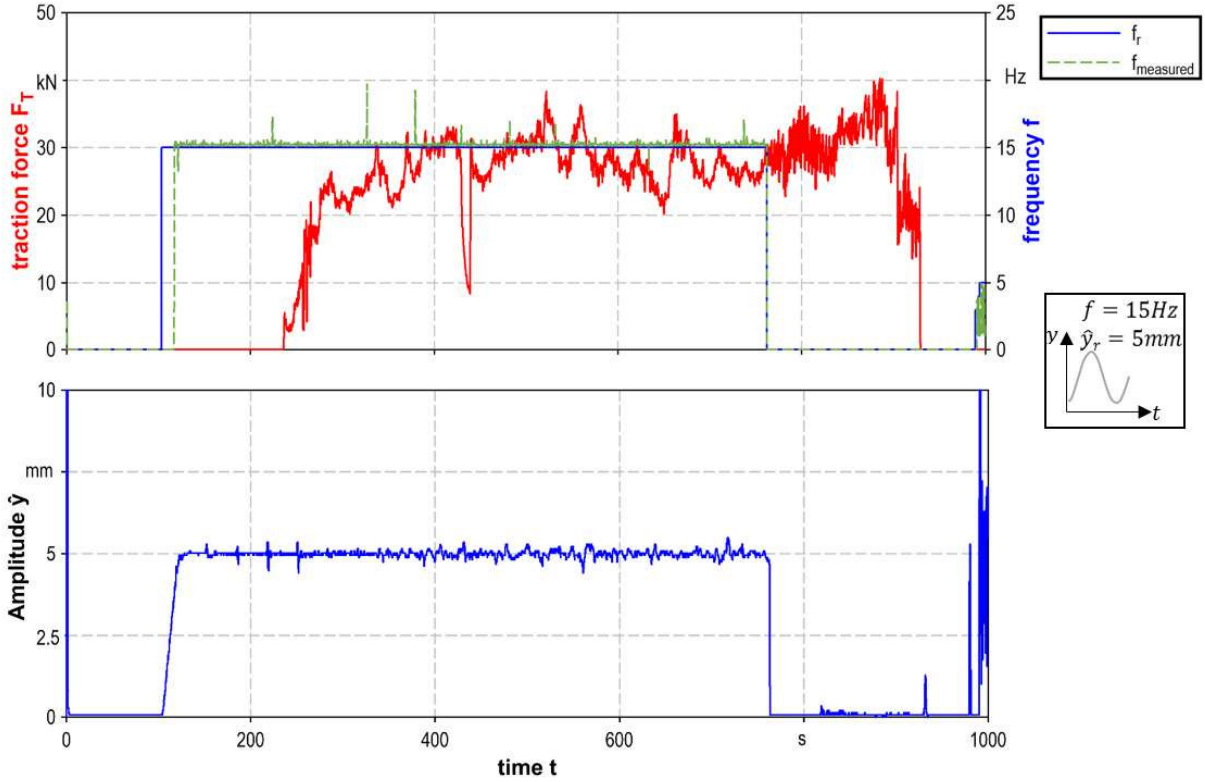

Figure 8: Comparison of traction forces with and without excitation

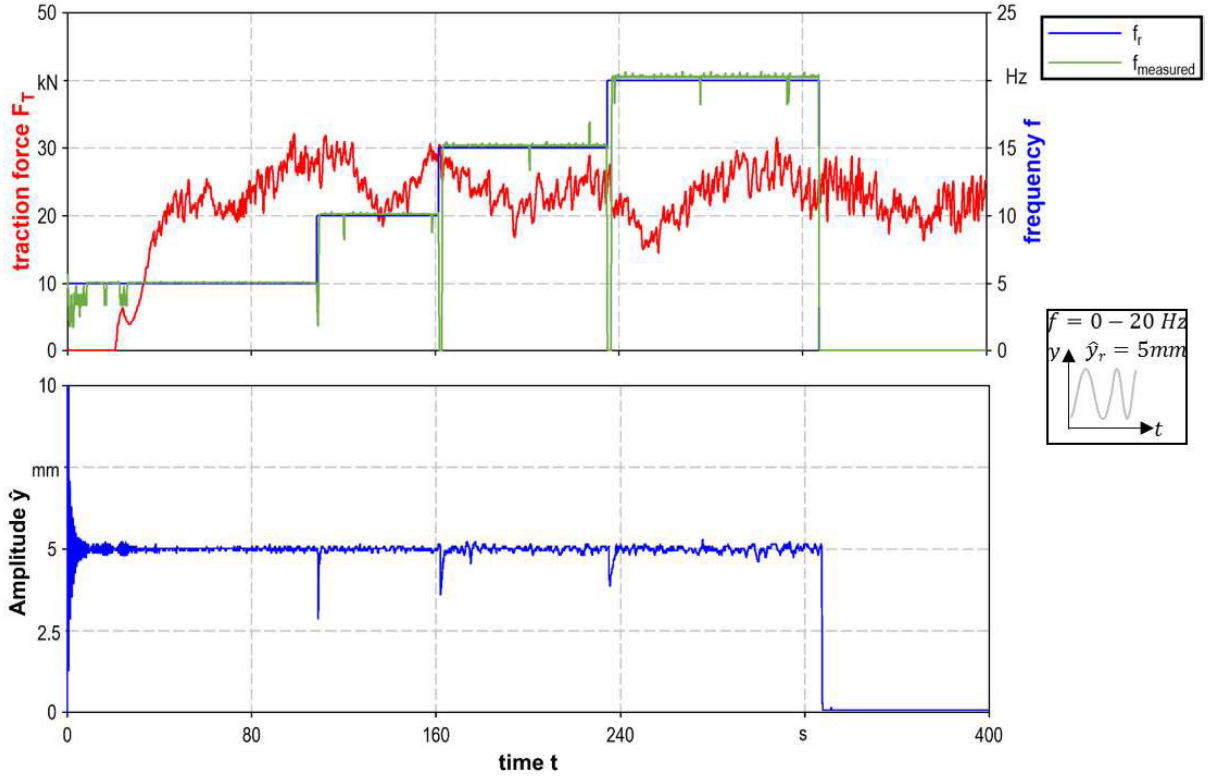

Figure 9: Comparison of traction forces at different frequencies

hundred percent evident that the traction force was reduced by change in frequency. The possible reasons are:

- Inadequate seal for the actuated vibration plough blade
- Unstable soil properties, especially caused by the multiple passes over the same route.
- Unstable driving behaviors, the speed of the tractor could not precisely been controlled for the low set-speed
- Limited vibration amplitude and cylinder force of the proposed system yields to no reaction of the soil yet
- Inappropriate vibration frequency, compared with resonant frequency of soil

6. CONCLUSION AND OUTLOOK

In this study, the linearized mathematical model for the hydraulically actuated vibration plough blade has been presented and used to qualitative analyse. In addition, the novel Co-Simulation with OPC UA aided in tuning the controller and achieving the expected performance before the machine was integrated. The simulation and test results were in good agreement with each other, which demonstrated that the developed control strategy for the hydraulically actuated vibration plough blade was adequate for the mission. After plough integration and tractor tests, it was shown through comparison experiments that the traction force could potentially be reduced with the help of vibration plough blade.

According to the field tests, there are still a lot of problems to be solved. Firstly, with introduction of road roller, the unstable properties could be partially compensated. Secondly, in order to identify the unstable driving behaviors, it is necessary to acquire the actual driving speed, rotation speed and torque of diesel engine. For future work, it is advised that an intelligent self-tuning PID controller can be developed for the electro-hydraulic system with direct position feedback. Moreover, to reduce the pressure drop for control edge and realize higher frequency and cylinder force, it is considerable to replace the proportional valve with fast switching valves and employ multiple actuators.

NOMENCLATURE

α	Area ratio
a_i	Coefficients in denominator of transfer function
A_A	Piston area (mm^2)
B	Coefficient of flow rate ($l/(min \cdot mm \cdot \sqrt{bar})$)
b_i	Coefficients in numerator of transfer function

C_A Hydraulic capacity for port A (l/bar)
C_B Hydraulic capacity for port B (l/bar)
d Cylinder rod diameter (mm)
d_V Damping coefficient of proportional valve
$d_{\dot{y}}$ Damping coefficient (N·s/mm)
D Cylinder piston diameter (mm)
f Frequency (Hz)
$f_{measured}$ Measured frequency (Hz)
f_r Reference frequency (Hz)
f_V Natural frequency of proportional valve (Hz)
m_L Equivalent load mass (kg)
F Force (N)
F_L Load force (N)
F_T Traction force (N)
K_H Hydraulic gain coefficient (bar/(l/min))
K_{Lep} Leakage-pressure-coefficient ((l/min)/bar)
$K_{Le\dot{y}}$ Leakage-velocity-coefficient ((l/min)/(mm/s))
K_M Mechanic gain coefficient (mm/(N·s))
K_{pA} Flow rate-pressure-coefficient for port A ((l/min)/mm)
K_{pB} flow rate-pressure-coefficient for port B ((l/min)/mm)
K_V Coefficient between voltage and displacement of valve spool (mm/V)
K_x Gain for displacement of valve spool (bar/(min·mm))
K_{xA} Flow rate - displacement of valve spool - coefficient for port A ((l/min)/mm)
K_{xB} Flow rate - displacement of valve spool - coefficient for port B ((l/min)/mm)
$K_{\dot{y}}$ Gain for velocity of cylinder (mm^2·bar/l)
p_0 System pressure (bar)
p_A Pressure in cylinder chamber A (bar)
p_{A0} Pressure in cylinder chamber A in hydraulic zero point (bar)
p_B Pressure in cylinder chamber B (bar)
P_{B0} Pressure in cylinder chamber B in hydraulic zero point (bar)
p_L Load pressure (bar)
p_T Pressure in tank (bar)
Q_A Flow rate to port A (l/min)
Q_{A0} Flow rate to port A in hydraulic zero point (l/min)
Q_B Flow rate to port B (l/min)
Q_{Le} Leakage (l/min)
T Tank temperature (°C)
T_H Hydraulic time constant (s)
T_M Mechanic time constant (s)
T_0 Temperature (°C)
u Input voltage (V)
x_V Displacement of valve spool (mm)
y Displacement of cylinder (mm)
$\dot{y}$ Velocity of cylinder (mm/s)
$\ddot{y}$ Acceleration of cylinder (mm/s^2)
y_0 Mean displacement of cylinder (mm)
y_{max} Cylinder max. stroke (mm)
$\hat{y}$ Actual amplitude of cylinder (mm)
$\hat{y}_r$ Amplitude reference (mm)
$\hat{y}_{r,sim}$ Amplitude reference in simulation (mm)
$\hat{y}_{r,test}$ Amplitude reference in test (mm)

OPC UA Open Platform Communications Unified Architecture

REFERENCES

[1] Grosa, A (2018) Agrothermie - Minimal invasive Einrichtung von Geothermienetzen unter Landwirtschaftsflächen. 76. Internationale Tagung LAND.TECHNIK, Germany
[2] Pietruschka, D (2016) Vision 2020 – Die Plusenergiegemeinde Wüstenrot. Stuttgart Fraunhofer IRB Verlag
[3] Pietruschka, D (2013) Kalte Nahwärme: agrothermische Wärme - Versorgung einer Plusenergiesiedlung. Bauma 2013 TECHNIK
[4] Dresig, H., Fidlin, A. (2014) Schwingungen mechanischer Antriebssysteme – Modellbildung, Berechnung, Analyse, Synthese. 3rd edition, Berlin, Heidelberg, p. 449 et seq.
[5] Murrenhoff, H (2008) Servohydraulik – Geregelte hydraulische Antriebe. Shaker Verlag GmbH, p. 235
[6] Su, S.J, Zhu Y.Y, Li C.J, Tang W.X, Wang H.R (2019) Dual-valve parallel prediction control for an electro-hydraulic servo system. Science Progress 1-21
[7] Pan, D.L, Gu S.J, Guo G.Y, Kuang H.B, Zhong H, Gao F (2017) Co-simulation design and experimental study on the hydraulic–pneumatic-powered driving system of main steam and feed water isolation valves for CAP1400. Advances in Mechanical Engineering Vol. 9(8) 1-11
[8] Mahnke W, Leitner S.H, Damm M (2009) OPC Unified Architecture. 2009 Springer-Verlag Berlin Heidelberg
[9] Rinaldi J (2016) OPC UA Unified Architecture: The Everyman's Guide to the Most Important Information Technology in Industrial Automation. CreateSpace Indepen-dent Publishing Platform
[10] Lange J, Iwanitz F, Burke Th. J (2010) OPC: Von Data Access bis Unified Architecture. VDE Verlag Gmbh